Materials Science-Poland, Vol. 26, No. 4, 2008

Crystallization of amorphous Fe–Cr–B alloys investigated with high heating rates

P. KAMASA[1*], L.K. VARGA[1], P. MYŚLIŃSKI[2], S.G. RASSOLOV[3], V. MAKSIMOV[3], B. IDZIKOWSKI[4]

[1]Research Institute for Solid State Physics and Optics of Hungarian Academy of Sciences, 1525 Budapest, POB 49, Hungary

[2]Vacuum Technology Transfer Center, Technical University of Koszalin, 5-620 Koszalin, Poland

[3]Donetsk Institute for Physics and Engineering of National Academy of Sciences of Ukraine, R. Luksemburg Str. 72, 84114 Donetsk, Ukraine

[4]Institute of Molecular Physics, Polish Academy of Sciences, M. Smoluchowskiego 17, 60-179 Poznań, Poland

Rapid annealing of metallic glasses results in their physical properties different from those stemming from isothermal or non-isothermal annealing with slow heating rates. Differential thermal analysis (DTA) with heating rates up to 2500 K·min^{-1} was applied to investigate amorphous alloys of the composition $Fe_{85-x}Cr_xB_{15}$ (x = 0, 1, 5) in order to follow the crystallization process. The results have been compared with those obtained with the usual low heating rate processes available from the commercial DSC method. Simultaneously recorded high heating rates magnetic susceptibilities complement the thermal measurements and reveal an interesting phenomenon of suppression of the decomposition of the residual amorphous phase when the heating rates exceed 1250 K·min^{-1}, 550 K·min^{-1} and 250 K·min^{-1} for x =0, 1 and 5, respectively. Both, the high heating rate and the Cr addition facilitate the formation of nanostructure which is stable against a further decomposition.

Key words: *DTA; TMAG; high heating rate; crystallization kinetics; amorphous alloy*

1. Introduction

Heating of amorphous alloys leads to their crystallization and structural changes. The positions of crystallization peaks depending on the heating rates and kinetics of the process is usually analyzed based on the Kissinger plot [1, 2]. The crystallization

Corresponding author, e-mail: kamasa@szfki.hu

following closely the glassy transition is a diffusion controlled process [3]. This behaviour is observed in the isothermal or isochronal experiments with low heating rates not exceeding 80 K·min^{-1}. The question arises, how this diffusion controlled process evolves with the increasing heating rate, above 80 K·min^{-1}. Except some "quench-up" experiments with the effective heating rate of about 10^4–10^6 K·s^{-1} carried out on thin films [4] and amorphous ribbons [5, 6], there are no reported thermal analysis experiments using a controlled high heating rate above 500 K·min^{-1} [7].

In the present work, results of measurements with high heating rates controlled up to 2500 K·min^{-1} are presented. The model material of $Fe_{85-x}Cr_xB_{15}$ (x = 0, 1 and 5) was selected as a well known amorphous alloys studied by low heating rate DSC and other methods [8].

2. Experimental

We have developed a DTA attachment to the existent home-built thermomagnetometer (TMA) [9] enabling simultaneous DTA and TMA measurements with high heating rates. Feedback controlled electric current heats the furnace in the form of a platinum boat, where a ribbon sample is placed in one side of the boat. The other side is used as a reference for temperature measurements. The thermal effects are detected as the temperature difference between the sample and the reference sites. The value of 2500 K·min^{-1} was the highest heating rate with feedback control of linearity (Fig. 1).

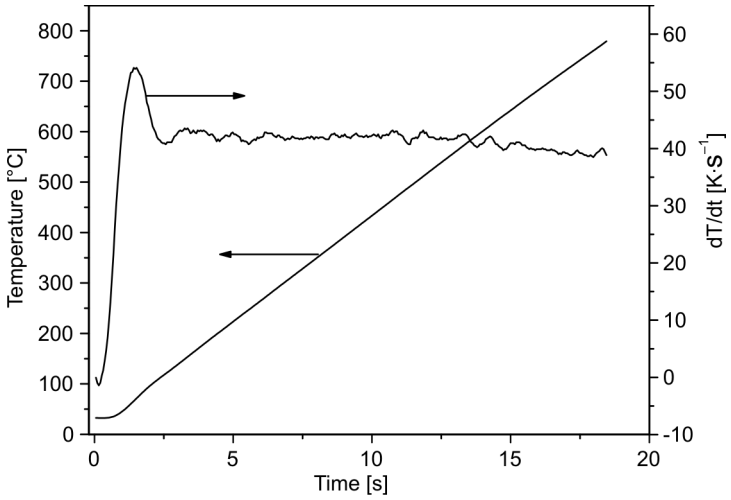

Fig. 1. Time dependence of temperature and its derivative recorded at the controlled rate of 2500 K·min^{-1}

Samples from a series of amorphous $Fe_{85-x}Cr_xB_{15}$ alloys with x = 0, 1, and 5 were prepared by the melt-spinning technique in the form of 1 mm wide and 20 μm thick

ribbons. The glassy state of the samples was confirmed by the X-ray diffraction measurements. The chemical composition of the material was analyzed by the atomic absorption spectroscopy. Two pieces of 10 mm long ribbons (altogether about 3 mg) was used in the DTA experiment. A similar amount of the material cut into 3 mm pieces was used in the DSC experiment.

3. Results

In Figure 2, the DTA and TMAG curves for $Fe_{85}B_{15}$ amorphous sample obtained using the heating rates between 700 and 2500 K·min^{-1}are plotted. The DTA signal was normalized with the heating rate in order to obtain comparable intensities. A two-stage crystallization is observed up to the heating rate of 1250 K·min^{-1}. The first exothermic peak (I) in the DTA and the increase of the magnetization value in the TMAG curve are attributed to the precipitation of α-Fe [11]. Next the residual amorphous phase enriches in boron and crystallizes eutecticallly into α-Fe + Fe_3B, and this process is observed as a second exothermic peak (II) in the DTA thermograph. A comprehensive analysis of the described above processes can be found elsewhere [8].

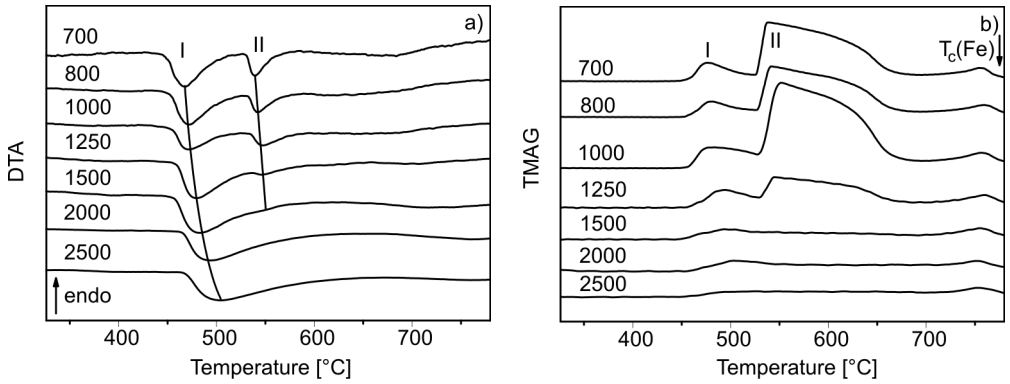

Fig. 2. Devitrification process of amorphous $Fe_{85}B_{15}$ alloy obtained at various heating rates as indicated: DTA curves from the crystallization region (a), and corresponding TMAG curves (b)

With the heating rate increasing above 1250 K·min^{-1}, only a smeared out one stage transformation (peak I) is recorded. The same tendency is observed in TMAG measurements results. The intensity of the magnetization corresponding to Fe_3B formation (peak II) is nearly equal to the first peak (I) of α-Fe precipitation at heating rates below 1000 K·min^{-1}. Above this value the peak II decreases together with the magnetization upraise of the first peak. Above 1500 K·min^{-1} heating rate, a smeared out first magnetization peak is only observed (Fig. 2b). Taking the peak temperatures, T_p, at a certain heating rate, q, an $\ln(q/T_p^2)$ versus $1/T_p$ Kissinger plot can be constructed, from which the activation energy of the process can be calculated. The above described

experiment was repeated also for two additional $Fe_{85-x}Cr_xB_{15}$ samples, where 1 at. % and 5 at. % of Fe was replaced by Cr. The Kissinger plots are presented in Fig. 3.

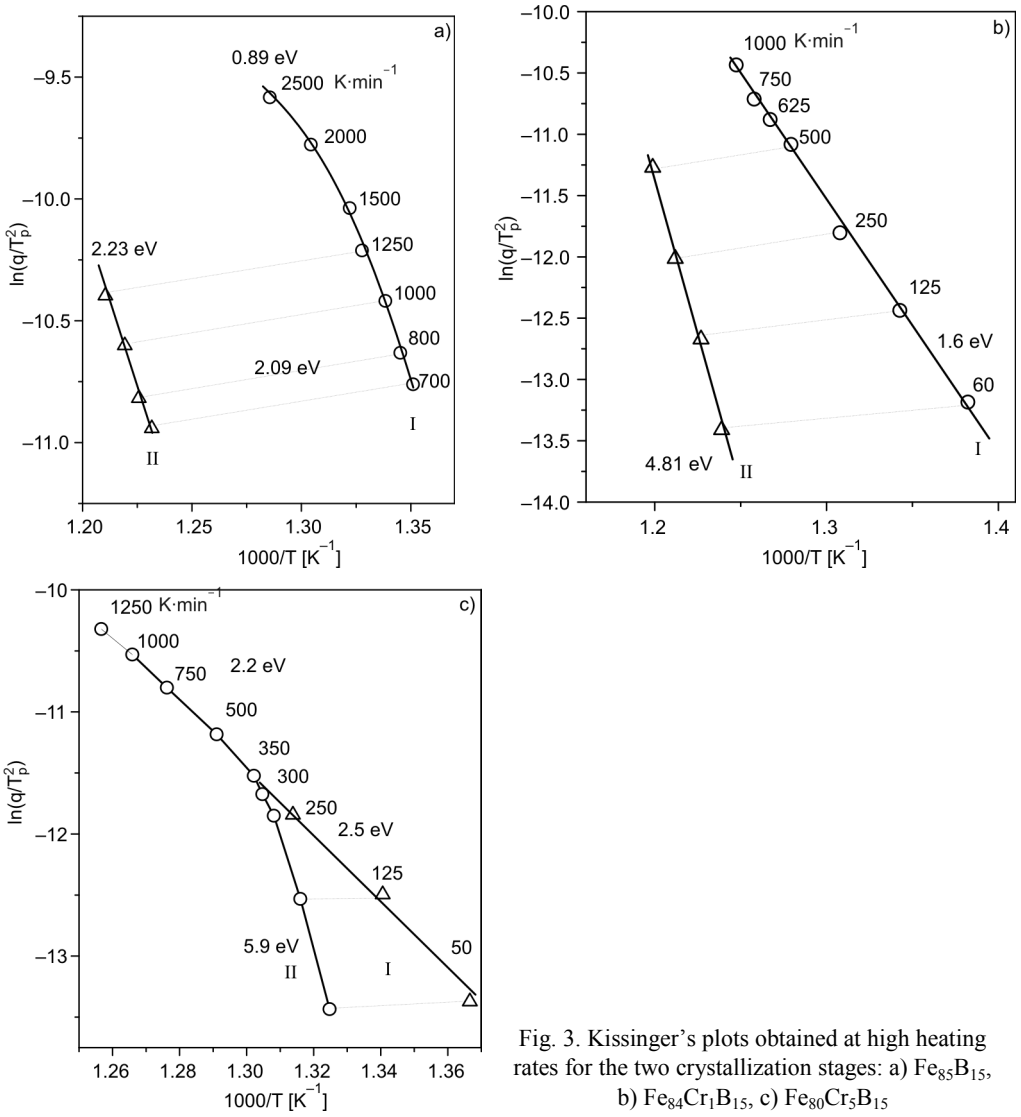

Fig. 3. Kissinger's plots obtained at high heating rates for the two crystallization stages: a) $Fe_{85}B_{15}$, b) $Fe_{84}Cr_1B_{15}$, c) $Fe_{80}Cr_5B_{15}$

The two crystallization stages of $Fe_{85}B_{15}$ are characterized by nearly the same activation energies, about 200 kJ/mol for each. With the increasing heating rate, the intensity of the higher temperature peak (II) decreases (Fig. 2), and finally it is immersed in the wider peak (I) at about 1250 $K \cdot min^{-1}$. At higher heating rates, above 1500 K min^{-1}, the plot corresponding to the lower temperature peak (I) clearly deflects from the linear behaviour. The 1 at. % Cr addition does not change the two-step character

of the crystallization process; however, the second peak dies out at a much lower heating rate (at about 500 $K \cdot min^{-1}$) than in the case of the original binary alloy $Fe_{85}B_{15}$.

The evolution of crystallization steps changes drastically when 5 at. % of Fe is replaced by Cr. The two-stage crystallization is only observed at low heating rates, below 250 $K \cdot min^{-1}$. With the increasing heating rate, the shift of the higher temperature peak (II) is smaller (higher activation energy) than that of the peak (I). At about 300 K/min the two peaks overlap and at higher heating rates only one peak is observed. This peak represents two processes: first, the precipitation of α-Fe, and second, further transformation of the residual amorphous phase. The slope of the overlapped process remained the same as of the process (I), indicating that the precipitation of α-Fe is the determining factor in the cooperative processes of the overlapping crystallization steps. While the activation energy of lower temperature peaks (I) does not change significantly for all three investigated alloys (ca. 220 $kJ \cdot mol^{-1}$), the activation energy for higher temperature peaks (II) increases with Cr content. For 1 and 5 at. % Cr contents, the values are 465 and 570 $kJ \cdot mol^{-1}$, respectively, in comparison with the value obtained for the pure binary alloy, amounting to 216 $kJ\ mol^{-1}$.

3. Discussion

High heating rates reveal new effects, which may originate directly in the devitrification processes. Remarkable is for instance, the deflection from the linearity of the Kissinger plot for the low temperature peak (I) of $Fe_{85}B_{15}$ above 1250 $K \cdot min^{-1}$ heating rates. High heating rates can involve higher temperature gradients within the sample, causing a widening in the temperature (time) range of crystallization and shifts the peak temperature, T_p, as well. In the devitrification process the primary crystallization of the α-Fe is a long-range diffusion process, which can be accomplished more easily (with smaller activation energies) at higher temperatures, resulted from the high heating rate shifting. On the other hand, the crystallization of the residual amorphous phase is a short- range diffusion process for which the activation energy is higher and seemingly does not change in the temperature interval of the peak shifting.

Another explanation of this phenomenon could be given by accounting the changes of the boron content in the α-Fe phase. As has been recently shown [12], the concentration of boron in the primary α-Fe increases from 0.14 to 0.39 with increasing the annealing temperature of the $Fe_{85}B_{15}$ metallic glass from 628 to 667 K. According the level rule, the volume fraction occupied by the primary crystals is proportional to [13]:

$$f_1 = \frac{c^* - c^0}{c^* - c^{xt}}$$

where c^* and c^0 are the matrix concentrations at the interface and far from it, respectively, and c^{xt} is the concentration of the crystallite precipitate. It is easy to show that at $c^{xt} \to c^0$ (i.e., to 0.15) the volume fraction of the α-phase approaches 1. In fact, the sample of amorphous $Fe_{85}B_{15}$ alloy crystallized at the heating rate of about 10^4 $K \cdot s^{-1}$

had a single phase structure consisting of nanoscale (10–30 nm) grains of supersaturated solid solution of boron in α-Fe [6]. Analysis of primary crystallization kinetics at high heating rates and structure of the partially (nanocrystalline states) and fully crystallized samples confirm this scenario of structural changes.

4. Conclusions

The behaviour of the crystallization steps in function of heating rates and Cr content revealed that the decomposition of the residual amorphous phase is strictly dependent on the evaluation of the first stage of the devitrification process. The calculations of activation energies of thermally activated reactions studied during linear heating confirm validity of model-free isoconversion methods which use approximations of the temperature integral [14]. As in the present case, these methods neglect the temperature integral at the start of the linear heating. A high rate of heat treatment may produce various nanostructures, not available at heat treatment with conventional low heating rates. This may cause disappearance of the higher temperature peak (II) observed with the increasing heating rate. XRD and TEM measurements (not presented here) confirm two different dynamics of structural changes.

References

[1] KISSINGER H.E., J. Res. Nat. Bureau Standards, 57 (1956), 217.
[2] KISSINGER H.E., Anal. Chem., 29 (1957), 1702.
[3] NAKAJIMA T., KITA E., INO H., J. Mater. Sci., 23 (1988), 1279.
[4] ADAMOVSKY S., SCHICK C., Thermochim. Acta, 415 (2004), 1.
[5] ZAŁUSKA A., MATYJA H., J. Mater. Sci. Lett., 2 (1983), 729.
[6] ABROSIMOVA G.E., ARONIN A.S., STELMUH V.A., Solid State Phys., 33 (1991), 3570.
[7] ICHITSUBO T., MATSUBARA E., NUMAKURA H., TANAKA K., NISHIYAMA N., TARUMI R., Phys. Rev. B, 72 (2005), 052201.
[8] KÖSTER U., HEROLD U., [in:] *Glassy Metals I*, H.J. Güntherodt, H. Beck (Eds), Springer, New York, 1981, 230.
[9] KAMASA P., VARGA L.K., KISDI-KOSZÓ É., VANDLIK J. [in:] P. Duhaj, P. Mrafko, P. Svec (Eds.), Suppl. to the Proc. 9th Int. Conf. on Rapidly Quenched and Metastable Alloys, Bratislava (Slovakia), 1996, Elsevier, Amsterdam, 1997, 280.
[10] KISDI-KOSZÓ É., KISS L.F., VARGA L.K., KAMASA P., Mater. Sci. Eng. A, 226–228 (1997), 689.
[11] KAMASA P., BUZIN A., PYDA M., KOVAC J., CZIRÁKI Á., LOVAS A., BAKONYI I., J. Magn. Magn. Mater, 257 (2003), 274.
[12] TKATCH V.I., RASSOLOV S.G., MOISEEVA T.N., POPOV V.V., J. Non-Cryst. Solids, 1351, (2005), 1658.
[13] CLAVAGUERA-MORA M.T., CLAVAGUERA N., CRESPO D., PRADELL T., Progr. Mater. Sci., 47 (2002), 559.
[14] STARINK M.J., Thermochim. Acta, 404 (2003), 163.

Received 31 May 2007
Revised 22 December 2007